The 1.48 Å Resolution Crystal Structure of the Homotetrameric Cytidine Deaminase from Mouse ‡

ARTICLE *in* BIOCHEMISTRY · JULY 2006

Impact Factor: 3.02 · DOI: 10.1021/bi060345f · Source: PubMed

6 AUTHORS, INCLUDING:

Aik Hong Teh
Universiti Sains Malaysia
8 PUBLICATIONS **62** CITATIONS

SEE PROFILE

Makoto Kimura
Nagoya University
94 PUBLICATIONS **2,156** CITATIONS

SEE PROFILE

Takashi Kumasaka
Japan Synchrotron Radiation Research Instit…
146 PUBLICATIONS **7,103** CITATIONS

SEE PROFILE

The 1.48 Å Resolution Crystal Structure of the Homotetrameric Cytidine Deaminase from Mouse‡

Aik-Hong Teh,§ Makoto Kimura,|| Masaki Yamamoto,⊥ Nobuo Tanaka,§ Isamu Yamaguchi,|| and Takashi Kumasaka*,§

Department of Life Science, Tokyo Institute of Technology, 4259-B-6 Nagatsuta-cho, Midori-ku, Yokohama, Kanagawa 226-8501, Japan, RIKEN, 2-1 Hirosawa, Wako, Saitama 351-0198, Japan, and RIKEN Harima Institute, RIKEN SPring-8 Center, 1-1-1 Kouto, Sayo, Hyogo 679-5148, Japan

Received February 19, 2006; Revised Manuscript Received May 2, 2006

ABSTRACT: Cytidine deaminase (CDA) is a zinc-dependent enzyme that catalyzes the deamination of cytidine or deoxycytidine to form uridine or deoxyuridine. Here we present the crystal structure of mouse CDA (*Mm*CDA), complexed with either tetrahydrouridine (THU), 3-deazauridine (DAU), or cytidine. In the *Mm*CDA−DAU complex, it clearly demonstrates that cytidine is distinguished from uridine by its 4-NH_2 group that acts as a hydrogen bond donor. In the *Mm*CDA−cytidine complex, cytidine, unexpectedly, binds as the substrate instead of the deaminated product in three of the four subunits, and in the remaining subunit it binds as the product uridine. Furthermore, the charge-neutralizing Arg68 of *Mm*CDA has also exhibited two alternate conformations, I and II. In conformation I, the only conformation observed in the other structurally known homotetrameric CDAs, Arg68 hydrogen bonds Cys65 and Cys102 to modulate part of their negative charges. However, in conformation II the side chain of Arg68 rotates about 130° around the Cγ−Cδ bond and abolishes these hydrogen bonds. The lack of hydrogen bonding may indirectly weaken the zinc−product interaction by increased electron donation from cysteine to the zinc ion, suggesting a novel product-expelling mechanism. On the basis of known structures, structural analysis further reveals two subclasses of homotetrameric CDAs that can be identified according to the position of the charge-neutralizing arginine residue. Implications for CDA−RNA interaction have also been considered.

Cytidine deaminase (CDA;[1] EC 3.5.4.5) is a zinc-dependent enzyme involved in the pyrimidine salvage pathway, catalyzing the hydrolytic deamination of cytidine or deoxycytidine into uridine or deoxyuridine (*1*, *2*) (Figure 1a).

On the basis of the CDA crystal structures from *Escherichia coli* (*3*) and *Bacillus subtilis* (*4*), CDA has been classified into homodimeric and homotetrameric forms. The homodimeric CDA, represented by *E. coli* CDA (*Ec*CDA) and *Arabidopsis thaliana* CDA (*5*), has one histidine and two cysteine residues liganding the zinc ion at the active site. On the other hand, the three zinc ligands of the homotetrameric CDA, which includes *B. subtilis* CDA (*Bs*CDA) and human CDA (*Hs*CDA) (*1*, *6*), are all cysteine residues. The two subunits of the homodimeric *Ec*CDA, each containing a zinc-bound catalytic domain and a noncatalytic C-terminal domain, form a pseudotetramer. The noncatalytic domain, although structurally homologous to the catalytic domain and the homotetrameric subunits, does not bind any zinc ion and has been proposed to evolve from a gene duplication of an ancestral homotetrameric CDA (*3*).

The homotetrameric CDA with an extra cysteine residue liganding the zinc ion has an arginine residue, as shown by Arg56 of *Bs*CDA (*4*), partially neutralizing the negative charge by hydrogen bonding two of the three cysteines. Arg56 has been proven to be important as mutating it to glutamine or alanine reduces the V_{max} (*7*). In addition to *Bs*CDA, two other CDA-related deaminases with three zinc-liganding cysteine residues, yeast RNA-editing deaminase *Sc*CDD1 (*8*) and *Aspergillus terreus* blasticidin S deaminase (*At*BSD; PDB codes 1WN5 and 1WN6), can also be grouped as homotetrameric CDAs on the basis of their structural similarities. While *At*BSD deaminates specifically blasticidin S (*9*), *Sc*CDD1 has been reported to also edit apolipoprotein B mRNA besides free cytidine, although the mRNA-editing mechanism of this enzyme still remains unclear (*10*).

We present here the structure of mouse CDA (*Mm*CDA), a homotetrameric CDA, complexed with either the inhibitors tetrahydrouridine (THU) and 3-deazauridine (DAU) or the substrate cytidine (Figure 1a). The enzyme−substrate structure has been made possible under the conditions employed in the crystallization. The 1.48 Å resolution structure of the *Mm*CDA−THU complex has also provided some interesting structural details previously not observed in the other homotetrameric CDAs, with implications for a potential product dissociation mechanism.

MATERIALS AND METHODS

Enzyme Expression and Purification. *Mm*CDA was cloned into the pET-21c vector (Novagen), and the resulting vector was transformed into *E. coli* cell strain BL21. The cells were

‡ The structures have been deposited in the Protein Data Bank as entries 2FR5, 1ZAB, and 2FR6 for the *Mm*CDA−THU, *Mm*CDA−DAU, and *Mm*CDA−cytidine complexes, respectively.

* To whom correspondence should be addressed. Telephone/Fax: (+81) 45 924 5707. E-mail: tkumasak@bio.titech.ac.jp.

§ Tokyo Institute of Technology.

|| RIKEN.

⊥ RIKEN Harima Institute.

[1] Abbreviations: CDA, cytidine deaminase; THU, tetrahydrouridine; DAU, 3-deazauridine; BSD, blasticidin S deaminase; DAC, 3-deazacytidine; apoB, apolipoprotein B; RMSD, root mean square deviation.

10.1021/bi060345f CCC: $33.50
Published on Web 06/01/2006

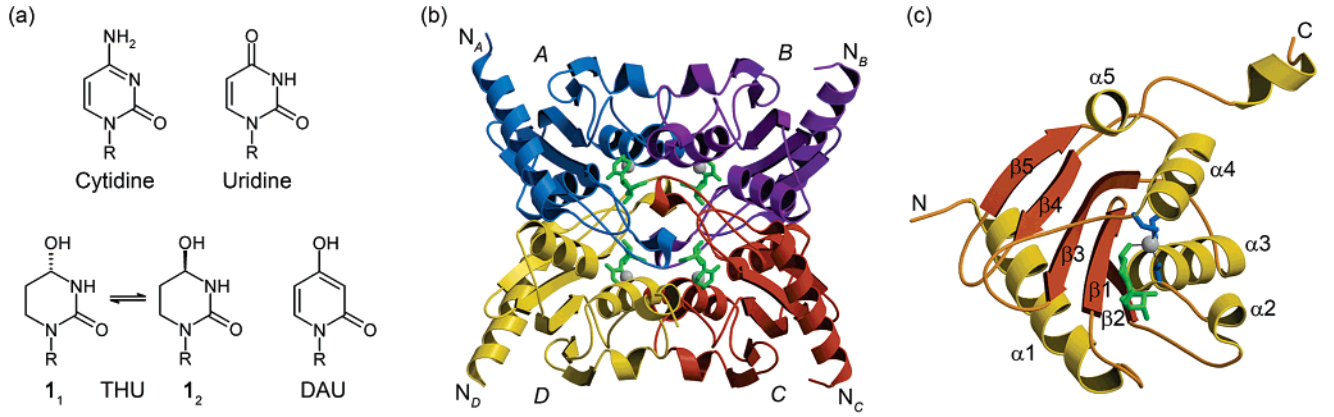

FIGURE 1: (a) Cytidine and deoxycytidine are converted to uridine and deoxyuridine by CDA, whereas tetrahydrouridine (THU) and 3-deazauridine (DAU) inhibit the reaction. THU exists in two epimers, $\mathbf{1}_1$ and $\mathbf{1}_2$. R denotes ribose, as well as deoxyribose in the case of cytidine and uridine. (b) The homotetramer of *Mm*CDA−THU, colored with subunits A, B, C, and D in blue, violet, red, and yellow. Zinc ions are shown as gray spheres, and THU in green stick representation. (c) The subunit of *Mm*CDA−THU, with the three zinc ligands shown in blue stick representation.

grown at 37 °C in LB supplemented with 50 μg/mL ampicillin. *Mm*CDA expression was induced during late exponential growth with 1 mM isopropyl β-D-thiogalactopyranoside (IPTG). After an overnight incubation with vigorous shaking, the cells were harvested and lysed in 20 mM Tris-HCl and 1 mM DTT, pH 7.5, by sonication and centrifuged. The supernatant was loaded onto a DEAE-650M column (TOYOPEARL), and *Mm*CDA was eluted stepwise with up to 60 mM NaCl. After dialysis, fractions containing *Mm*CDA were subjected to Mono Q chromatography (Pharmacia) with gradient elution at 0−200 mM NaCl. The active fractions were concentrated and further gel-filtrated on a Superdex 75 column (Amersham).

Crystallization. Crystallization screening with Crystal Screen (Hampton Research) yielded stacking crystals in solution 4 (2.0 M ammonium sulfate, 0.1 M Tris-HCl, pH 8.5). Using the hanging drop vapor diffusion technique, the crystals were subsequently grown at 25 °C in drops containing 1.5 μL of 10−15 mg/mL *Mm*CDA (20 mM Tris-HCl, 1 mM DTT, pH 7.5) and 5 mM THU, DAU, or cytidine, mixed with 1.5 μL of an optimized mother liquor (0.8−1.0 M ammonium sulfate, 0.1 M citrate, pH 3.8−4.5). Crystals of the *Mm*CDA−THU complex appeared after a few hours, while the other two complexes took several days.

Data Collection. Diffraction data were collected under cryogenic conditions (100 K) on a Rigaku/MSC Jupiter210 CCD detector at beamline BL26B2, SPring-8, Japan, for the THU and DAU complexes and on a Rigaku RU300 rotating anode generator with a Rigaku RAXIS IV image plate detector for the cytidine complex. The crystals were soaked in mother liquor containing 20% glycerol and flash frozen prior to data collection. Data were processed with the Rigaku CrystalClear software. All of the three crystals belong to space group *I*222.

Structural Determination and Refinement. The structure of *Mm*CDA−THU was solved by molecular replacement using Molrep (*11*) with *Hs*CDA (PDB code 1MQ0) as a search model. The result yielded a model with four subunits related by *222* symmetry. Refinement using CNS (*12*) was alternated with model building using Xfit of XtalView (*13*), and during several rounds of these the inhibitor THU as well as water molecules was added into the model, followed by a number of alternate conformations further down the refinement routine. The finished *Mm*CDA−THU structure was used as the initial model for the determination of both the *Mm*CDA−DAU and *Mm*CDA−cytidine structures. The inhibitor DAU was introduced into the *Mm*CDA−DAU model without much difficulty, but in the *Mm*CDA−cytidine model electron density showed two types of ligand binding, interpreted as cytidine in three of the subunits and uridine in the other. A peak of electron density bulging from uridine C4 was also clearly observed, but since the pyrimidine moiety of neither a mixture of cytidine and uridine at half-occupancy nor an intermediate with bonded O4 and N4 could fit properly into the electron density, it was modeled as uridine with an ammonia molecule. Because of their lower resolutions, alternate conformations for only Arg68 and Lys73 were introduced into these two models. In the final stage, a sulfate ion lying on a special position was included in all three models, and *B*-values were also refined. The structure of *Mm*CDA−THU was further refined with TLS (*14*) using Refmac (*15*). The data collection and refinement statistics are summarized in Table 1.

Table 1: Data Collection and Refinement Statistics

data set	*Mm*CDA−THU	*Mm*CDA−DAU	*Mm*CDA−cytidine
	Data Collection		
space group	*I*222	*I*222	*I*222
cell dimensions			
a (Å)	82.24	82.24	82.20
b (Å)	93.40	92.36	92.96
c (Å)	180.74	180.53	180.74
no. of unique reflections	111799	28544	42537
resolution (Å)	41.49−1.48 (1.53−1.48)	48.56−2.36 (2.44−2.36)	33.59−2.07 (2.14−2.07)
completeness (%)	96.7 (98.9)	99.4 (100.0)	100.0 (99.9)
R_{merge} (%)	7.3 (28.8)	9.5 (29.0)	7.9 (34.5)
$\langle I/\sigma \rangle$	15.6 (5.0)	9.8 (4.4)	11.4 (3.9)
	Refinement[a]		
no. of reflections	111795	28184	42417
R_{work} (%)	16.8	17.6	18.8
R_{free} (%)	19.0	20.6	21.4
average *B*-factor (Å^2)	13.6	23.2	25.6
RMSD			
bond length (Å)	0.009	0.005	0.005
bond angle (deg)	1.4	1.3	1.4

[a] Values in parentheses are for the highest resolution shell.

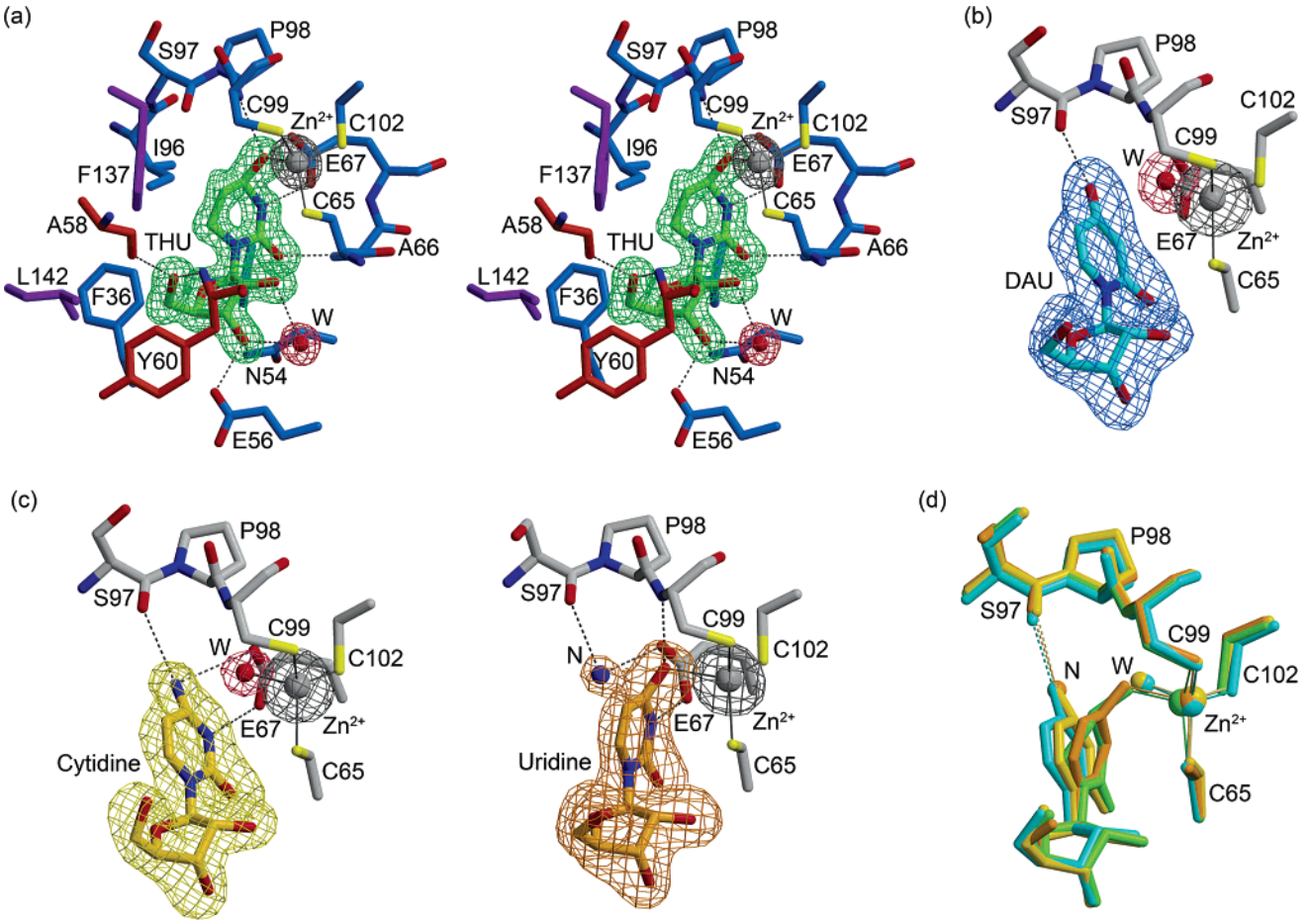

FIGURE 2: Binding modes of the inhibitors and substrate. (a) Stereoview of the zinc-bound THU in subunit A. Residues from subunits A, B, and C are colored blue, violet, and red. The zinc ion and the water molecule are shown as gray and red spheres. Zinc binding is shown as solid lines, and hydrogen bonds are shown as dotted lines. (b) DAU binds with its 4-OH group hydrogen bonded to the backbone O of Ser97. (c) In the *Mm*CDA−cytidine complex, while cytidine binds as the substrate in three of the subunits (left), in the remaining subunit it binds as the product uridine (right), with the leaving ammonia molecule (N) shown as a blue sphere clearly visible in the electron density. (d) Superposition of the binding structures of THU (green), DAU (blue), cytidine (yellow), and uridine (orange). The $F_o - F_c$ omit maps are contoured at 6.0σ for THU, 4.5σ for DAU, cytidine, and uridine, and 10.0σ for all of the zinc ions.

Others. The multiple sequence alignment was constructed with ClustalW (*16*), and edited manually with the program Indonesia (http://xray.bmc.uu.se/dennis/). All figures were prepared with MOLSCRIPT (*17*) and Raster3D (*18*), and the electron density maps in Figures 2 and 3 were output from Xfit.

RESULTS

Overall Structure. The *Mm*CDA structure exhibits a fold characteristic of the CDA family. All of the four subunits are related by *222* symmetry (Figure 1b) and superimposed well within an rmsd of 0.48 Å at the Cα atoms. Each subunit consists of a core of five β-strands (β1−β5), sandwiched by one α-helix (α1) on one side and three α-helices (α3−α5) on the other (Figure 1c). The subunit also binds a zinc ion and an inhibitor or a substrate at the active site. The central cavity formed by the four subunits is filled with solvent molecules.

About 10 residues of the N-terminus are disordered, and electron density for the last two and three C-terminal residues of subunits B and C is not well defined. Superposition of the four C-terminal regions shows that they diverge structurally beyond Gln43. This implies that the C-terminal region, which lies across the entrance of the adjacent active site cavity, is flexible and may control access to the active site. Side chains of Arg68 and Lys73, and in *Mm*CDA−THU more residues including Gln72, were modeled with alternate conformations.

Active Site and Substrate Binding. The active site is comprised collectively of residues from three subunits, with the catalytic zinc ion coordinated by Cys65, Cys99, and Cys102 in tetrahedral geometry (Figure 2a). Binding modes of both the inhibitors and the substrate are similar to those observed in other CDAs. The ribose ring is bound in a C2′-*endo* puckering mode, with the 3′-OH group hydrogen bonded not only to the side chains of the highly conserved Asn54 and Glu56 but also to a water molecule which also forms the only hydrogen bond with the 2′-OH group (Figure 2a). This type of interaction is not observed in the crystal structures of both *Ec*CDA and *Bs*CDA but is found in the *Hs*CDA structure, as well as the adenosine deaminase (ADA) structure (*19*). In ADA both the 2′- and 3′-OH groups of the ribose share a water molecule, but the ribose ring of adenosine assumes a C3′-*endo* ring pucker.

As also observed in the *Bs*CDA−THU complex (*4*), the zinc-bound THU is found in the epimer $\mathbf{1}_2$ form (Figures 1a and 2a), the predominant epimer in aqueous solution with an inhibitory activity about a factor of 13 higher than the

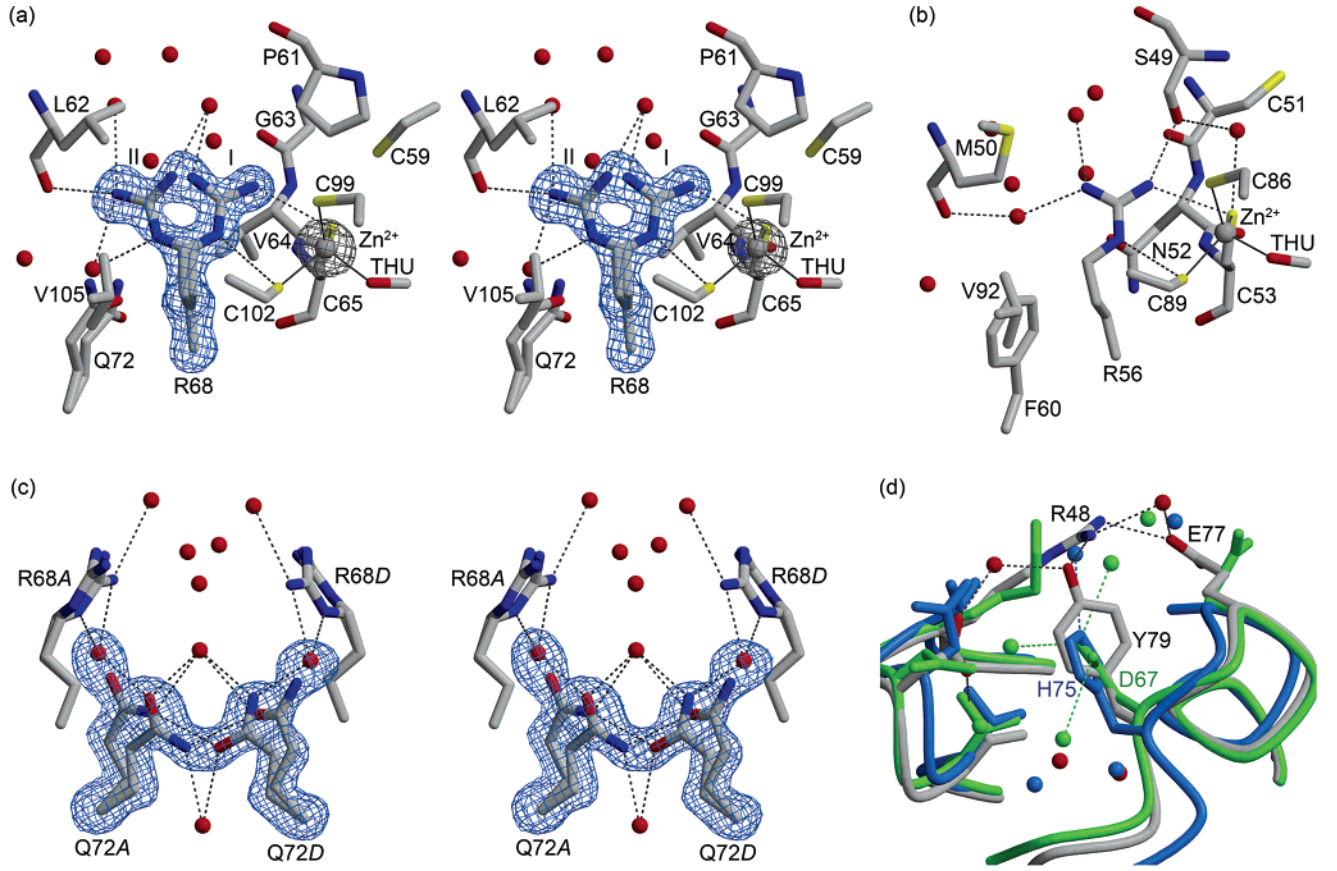

FIGURE 3: (a) Stereoview of *Mm*CDA Arg68. Arg68 is observed in two alternate conformations, I and II. In comparison, only conformation I is present for (b) *Bs*CDA Arg56. (c) The Gln72 dyad from subunits A and D of the *Mm*CDA−THU complex. The $F_o - F_c$ omit maps are contoured at 4.0σ for Arg68 and Gln72 and at 10.0σ for the zinc ion. (d) *Mm*CDA Tyr79, as well as *Sc*CDD1 His75 (blue), is exposed to the solvent. The corresponding residue of *Bs*CDA is a linear Asp67 (green).

other epimer $\mathbf{1}_1$ (*20*). The THU 4-OH group binds the zinc ion as the fourth ligand. By contrast, the DAU 4-OH group is bound to the backbone O of Ser97 in a binding mode similar to that observed in *Ec*CDA complexed with 3-deazacytidine (DAC) (*21*), with a water molecule acting as the fourth ligand of the zinc ion (Figure 2b).

In the *Mm*CDA−cytidine complex, as cytidine was added before crystallization it was expected to be deaminated and bind as uridine in the active site. Surprisingly, two binding modes were observed. In three of the four subunits, similar to the *Mm*CDA−DAU complex the expected uridine was bound to the backbone O of Ser97, with a water molecule binding as the fourth ligand of the zinc ion (Figure 2c, left). Since the O4 of uridine does not have a hydrogen to hydrogen bond Ser97, the expected uridine was instead modeled as the substrate cytidine that possesses a 4-OH group as a hydrogen bond donor. In the remaining subunit, on the other hand, the expected uridine was found binding to the zinc ion in a fashion identical to that of the *Es*CDA−uridine complex (*22*), but a bulge of electron density close to its C4 was also clearly observed (Figure 2c, right). A similar peak has also been observed in the *Es*CDA−uridine complex and was modeled as a water molecule among the three possible interpretations as an ammonia molecule, an ammonium ion, or a water molecule. In the *Mm*CDA−cytidine complex, this bulge spatially corresponded to the N4 of cytidine in the other three subunits (Figure 2d), and in the presence of concentrated ammonium sulfate (0.8 M) it could represent the outgoing ammonia which was formed but trapped in the reaction during crystallization. Since modeling with either including the Ser97 leaning cytidine or an intermediate with bonded O4 and N4 did not fit the electron density for the pyrimidine moiety, the possibility of either a mixture of cytidine and uridine or an intermediate was ruled out. In view of the close proximity of the bulge to the uridine, as well as its corresponding position to the cytidine N4 in the other three subunits, it was modeled as an ammonia molecule at 2.21 Å from uridine C4 (versus 2.79 Å in *Es*CDA−uridine) among other equally probable choices of an ammonium ion or a water molecule.

Alternate Conformations. Instead of the histidine in the homodimeric CDA, the homotetrameric CDA has an extra cysteine residue liganding the zinc ion and thus an additional negative charge. The nearby Arg56 of *Bs*CDA partially neutralizes the negative charge by hydrogen bonding to two of the three cysteines (*4*, *7*). However, in contrast to the single conformation of this arginine observed in *Bs*CDA, *Hs*CDA, and *Sc*CDD1, in all three of the *Mm*CDA complexes the corresponding Arg68 was modeled into two alternate conformations, referred to as I (*gauche*$^+$) and II (*gauche*$^-$) (Figure 3a). Nη1 and Nϵ of Arg68 in conformation I forms two hydrogen bonds with Cys65 and Cys102, but an approximate 130° clockwise rotation around the Cγ−Cδ bond into conformation II abolishes these hydrogen bonds. In conformation II, Arg68 Nη1 interacts with the backbone of Leu62 from the neighboring subunit. As excess electron density was observed for Arg68 Nη1 in both conformations in the 1.48 Å resolution structure of *Mm*CDA−THU

complex, this nitrogen atom was refined with unit occupancy, indicating the coexistence of a water molecule at the same site.

The high resolution of *Mm*CDA−THU also reveals extensive electron density for the nearby Gln72; hence alternate conformations were modeled into it with two such Gln72 from adjacent subunits forming a dyad across the subunit interface (Figure 3c). The side-chain amide groups of the dyad were fixed in opposite orientations so that Oϵ1 and Nϵ2 from the two respective residues could hydrogen bond to each other.

DISCUSSION

Binding Modes of the Inhibitors. On the basis of the structural studies of *Ec*CDA (*3*, *21*, *22*), it has been proposed that upon entering the active site of *Ec*CDA the 4-NH_2 group of cytidine is captured by the backbone O of Thr127. Glu104 then shuttles a proton from the zinc-bound hydroxyl ion to cytidine N3, pulling the pyrimidine moiety toward the zinc-bound ion and leaving the ammonia behind. Because N3 is substituted with carbon in the inhibitor 3-deazacytidine (DAC), in the *Ec*CDA−DAC complex DAC could not interact with Glu104, and hence the pyrimidine moiety remained bound to the ammonia-binding Thr127 (*21*). On the other hand, since uridine O4 is a hydrogen bond acceptor and cannot hydrogen bond the backbone O of Thr127, in the *Ec*CDA−uridine complex (*22*) uridine might have bound the zinc ion in a single step upon entering the active site, without the need for the pyrimidine moiety to be captured by Thr127 and then pulled toward the zinc ion.

The inhibitor 3-deazauridine (DAU, Figure 1a) possessing a 4-OH group could also possibly interact with the zinc ion in the same manner as uridine in the *Ec*CDA−uridine complex. However, the *Mm*CDA−DAU complex has instead revealed a DAU that behaves similarly as DAC, with its 4-OH group forming a hydrogen bond to the backbone O of Ser97 (Figure 2b). The 4-OH group must have been captured by Ser97 before it could interact with the zinc ion, and since DAU does not have an N3 to interact with Glu76, the pyrimidine moiety could not possibly be pulled toward the zinc-bound hydroxyl ion and hence remained bound to Ser97. From these results, it is obvious that in CDAs the substrate is recognized by a hydrogen bond donating group attached to the C4 of the pyrimidine moiety, which can interact with the backbone O of the ammonia-binding residue.

The predominant epimer $\mathbf{1}_2$ of THU observed in the *Mm*CDA−THU complex, however, has a 4-OH group spatially oriented toward the zinc ion so it could easily interact with the latter (Figure 2a). Although the 4-OH group of epimer $\mathbf{1}_1$ should also possibly bind Ser97 to form a complex like *Mm*CDA−DAU, this was not observed probably due to the predominance and higher stability of the epimer $\mathbf{1}_2$ (*20*).

MmCDA−Cytidine Complex. Since uridine does not possess a hydrogen bond donating group attached to its C4 and hence cannot bind the backbone O of Ser97, the expected uridine present in three of the four active sites of the *Mm*CDA−cytidine complex was considered, with surprise, not deaminated and instead bound as the substrate to Ser97 (Figure 2c, left). Nevertheless, this was possible because first the deamination of cytidine by CDA is a reversible reaction (*23*) and second a high concentration of ammonium sulfate (0.8−1.0 M) was present in the crystallization buffer. As cytidine was mixed with the enzyme solution before crystallization, all of the cytidine molecules were believed to have been deaminated into uridine before being converted back to cytidine in the active site during crystallization. Furthermore, the enzyme−substrate complex could also possibly be stabilized in the presence of a low pH (∼pH 4), under which condition CDA activity is greatly reduced (*1*). In comparison, under the same condition of 0.8 M ammonium sulfate but at pH 6.2, only the *Ec*CDA−uridine complex was observed when the ligand-free *Ec*CDA crystals were soaked with the substrate cytidine (*22*). However, it is notable that, under the crystallization condition for *Mm*CDA, cytidine *was* indeed deaminated in solution, albeit slowly (data not shown). Hence, besides a high concentration of ammonium sulfate at low pH, a closed active site of the enzyme was most probably also a prerequisite for the conversion of uridine into cytidine. It was likely that, in the wake of a uridine molecule having bound to the zinc ion, an ammonia molecule positioned itself into the ammonia-binding site before the active site closed for the enzymatic reaction to reverse. The *Mm*CDA−cytidine complex has demonstrated that, under the right conditions, a substrate could be trapped in the active site to provide a structural insight into how a reaction begins, although it is not known if it is true for both the reversible and irreversible reactions.

Surprisingly, in none but one of the four subunits the electron density was leaning toward the zinc ion; thus the expected uridine molecule was believed deaminated and bound as uridine with its O4 attached to the zinc ion (Figure 2c, right). Furthermore, electron density bulging from uridine C4 was also clearly defined, and it coincided with the position of cytidine N4 in the other three subunits. Taking into consideration that ammonia (or an ammonium ion) must have bound at this site for cytidine to be reversibly formed in the other subunits, as well as its close proximity to uridine C4, this bulge was interpreted as an ammonia molecule hydrogen bonded to Glu67 and Ser97, but somehow the reverse reaction never proceeded to completion. This heterogeneity was a very interesting but perplexing observation which was probably induced by crystal packing, as no major differences between this active site and the other three were observed except the uridine molecule had the lowest average of *B*-factors among the four ligands. If pH was an important factor in influencing the formation of either the substrate or the product in the active site, this complex would clearly demonstrate that the interior environment of a closed active site of a subunit could induce different pHs according to its packing in the asymmetric unit.

A Genuine MmCDA Arg68 with a Rotating Side Chain. In comparison to the homodimeric CDA, the homotetrameric CDA with three zinc-liganding cysteine residues is considered to contain an additional negative charge. This would likely decrease the reactivity of the zinc ion to activate a water molecule. In all of the presently known structures, the active site is located at the positive dipole of two α-helices (α3 and α4 in *Mm*CDA, Figure 1c) that partly modulate the negative charges of the cysteine residues. In addition, hydrogen bonds from nearby residues have also been proved to be important in neutralizing the negative charges, such as shown by studies on the highly conserved Arg56 of *Bs*CDA

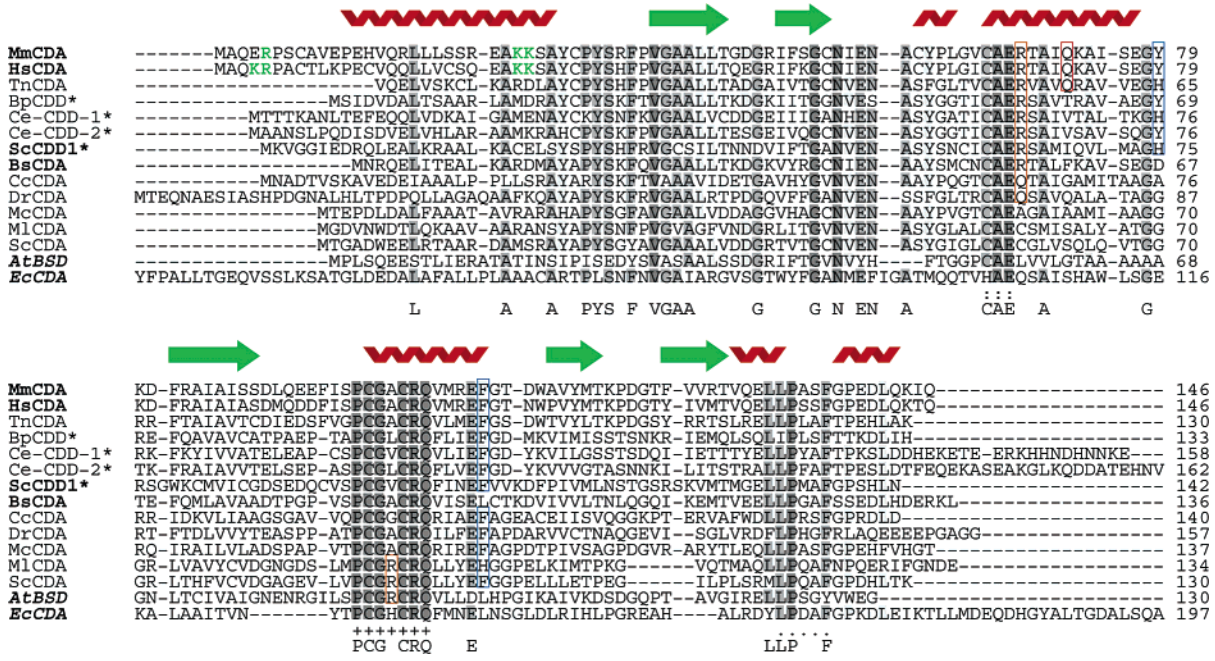

FIGURE 4: Sequence alignment of homotetrameric CDAs. Enzymes with solved structures are in boldface, and the conserved signature motifs C(H)AE, PCGXCRQ, and LPXXF are marked with (:), (+), and (.). Arginine (or glutamine) residues of the two subclasses of the homotetrameric CDA are boxed in orange, and the Glu72 dyad of *Mm*CDA is boxed in red. The four CDAs with proven RNA-interacting activity are marked with (*), and the two aromatic residues conserved in them but in neither *Ec*CDA nor *Bs*CDA are boxed in blue. Note that the first aromatic residue (tyrosine or histidine) is conserved only in some eukaryotic CDAs, compared to the more widely conserved second aromatic residue (phenylalanine or histidine). Residues from the putative bipartite NLS of *Hs*CDA and *Mm*CDA are printed in green. The homotetrameric CDAs are from *Mus musculus* (MmCDA; BAB25898), *Homo sapiens* (HsCDA; P32320), *Tetraodon nigroviridis* (TnCDA; CAG04590), *Brugia pahangi* (BpCDD; Q93143), *Caenorhabditis elegans* (Ce-CDD-1; AAB04993), *C. elegans* (Ce-CDD-2; AAB03151), *Saccharomyces cerevisiae* (ScCDD1; Q06549), *Bacillus subtilis* (BsCDA; P19079), *Caulobacter crescentus* (CcCDA; B87622), *Deinococcus radiodurans* (DrCDA; Q9RSE7), *Methylobacterium chloromethanicum* (McCDA; CAD20227), *Mycobacterium leprae* (MlCDA; CAC31129), and *Streptomyces coelicolor* (ScCDA; CAC33054). *Aspergillus terreus* blasticidin S deaminase (AtBSD; P78986) and the catalytic N-terminal domain of the homodimeric *Escherichia coli* CDA (EsCDA; P13652) are in italics.

that hydrogen bonds two of the three cysteine residues (*4*, *7*).

In *Mm*CDA, intriguingly, Arg68 which provides hydrogen bonding for Cys65 and Cys102 is unambiguously modeled into I (*gauche*$^+$) and II (*gauche*$^-$) alternate conformations (Figure 3a). The side chain of Arg68 is surrounded by all hydrophobic residues (Pro61, Leu62, Val64, Ala101, Val105) except Cys65, Gln72, and Cys102. Arg68 in conformation I hydrogen bonds the two cysteine residues, but rotating approximately 130° around the Cγ−Cδ bond into conformation II abolishes these hydrogen bonds altogether. In conformation II, Arg68 interacts with the backbone of Leu62 from the adjacent subunit, as well as indirectly with the Gln72 dyad through a water molecule (Figure 3c). The dyad is formed by two Gln72 residues, which is also conserved in *Hs*CDA and the freshwater pufferfish *Tetraodon nigroviridis* CDA (Figure 4), from two neighboring subunits interacting across the subunit interface. The side chain of Arg68 is directed to the solvent-filled interface of the four subunits, and Arg68 in both conformations also interacts with some water molecules. There is sufficient space for Arg68 to make a 130° clockwise rotation around the Cγ−Cδ bond from conformation I into conformation II, but a 230° anticlockwise rotation is sterically hindered by Ala101 and Val105 from the highly conserved PCGACRQV (both residues underlined) motif. Conformation II is seemingly detrimental, as mutating Arg56 of *Bs*CDA to glutamine or alanine has been shown to reduce its V_{max} (*7*). By abolishing the hydrogen bonds with the cysteine residues, conformation II could result in increased electron donation from the cysteine residues to the zinc ion, thereby weakening the ability of the zinc ion to activate a water molecule. On the other hand, however, the interaction between the zinc ion and the product uridine could also be weakened in a similar way, suggesting that the rotation of Arg68 may actually facilitate the release of the newly formed product.

In *Bs*CDA, the absence of conformation II for Arg56 may be due to crystal packing or the intrinsic lack of it. Nevertheless, structurally it can be explained by the influence of two residues, Ser49 and Asn52. Besides hydrogen bonding to Cys53 and Cys89, Arg56 is also firmly anchored to Ser49 (*4*) (Figure 3b). The side chain of Asn52 may also obstruct the clockwise rotation of Arg56 into conformation II, while an anticlockwise rotation is prevented by the PCGACRQV motif in a structurally similar fashion as that in *Mm*CDA. These two polar residues are replaced by hydrophobic residues in *Mm*CDA (Ser49 by Pro61 and Asn52 by Val64), hence eliminating their interactions with the side chain of Arg68. Moreover, the Gln72 dyad that indirectly interacts with conformation II is substituted with Phe60 in *Bs*CDA, which is also not well positioned for a π hydrogen bond with the Nϵ of Arg56 could it rotate into conformation II, and this further constitutes an unfavorable environment for conformation II.

The homotetrameric *Sc*CDD1 also has an identically positioned Arg64, present in only conformation I, for hydrogen bonding with Cys61 and Cys99 (*8*). This Arg64 is likewise anchored to the side chain of Ser57 and further to the backbone of Cys59. Together, these observations show that while in *Bs*CDA and *Sc*CDD1 the side chain of the

charge-neutralizing arginine residue is steadfastly positioned to hydrogen bond two of the three zinc-liganding cysteine residues, in *Mm*CDA this arginine has evolved into a flexible Arg68 that can make or break the hydrogen bonds by shifting its side chain from one conformation to another. Nevertheless, *Hs*CDA has not been modeled with its Arg68 in two alternate conformations (*6*) despite an 81% identity with *Mm*CDA. *Hs*CDA Arg68 is surrounded by the same residues in an identical environment as observed in *Mm*CDA, and the only exception is that Val64 of *Mm*CDA is replaced with Ile64. It is also plausible that, at 2.4 Å resolution, conformation II was not readily observable.

A Possible Product-Expelling Mechanism. Since uridine has a lower solubility than cytidine (*24*), an efficient mechanism for weakening the O4−zinc bond upon product formation, and subsequently expelling the uridine molecule into the solvent, might be critical in maintaining the catalytic activity of CDA. In the homodimeric *Ec*CDA−uridine complex, the N1−C1′ glycosidic bond of uridine is distorted about 19° out of the ribose plane, and this has been proposed as a means for weakening the O4−zinc bond, "spring-loading" the product complex and promoting product release (*22*).

The present data of *Mm*CDA, however, have suggested another unique way of modulating the zinc reactivity for water activation and product release by employing the alternate conformations of Arg68. Arg68 in conformation I, hydrogen bonding to Cys65 and Cys102 (Figure 3a) as was in *Bs*CDA, could help to enhance the net positive charge of the zinc ion in order to maintain a low pK_a for the zinc-bound water. Once the substrate was deaminated and the product was formed, the side chain of Arg68 might rotate into conformation II, breaking the hydrogen bonds with the two cysteine residues. Although a water molecule might occupy the site evacuated by Arg68 Nη1, as indicated by the extra electron density observed around Arg68 Nη1 in both conformations when refined with half-unit occupancy, this water molecule could hydrogen bond only Cys65 but not Cys102. Furthermore, a transient state might exist wherein Arg68 had broken all hydrogen bonds but the water molecule had yet to enter the site and establish its own, leaving both cysteine residues transiently not hydrogen bonded. The electrostatic environment of the zinc ion during this state would hence become more negative due to increased electron donation from the cysteine residues, resulting in a destabilized product−zinc transition complex and subsequently product dissociation.

However, what would have propelled the rotation of the Arg68 side chain into one or the other conformation is unclear. The nearby Gln72 dyad, also modeled with alternate conformations (Figure 3c), might seesaw together between the two conformations with one of them in the first conformation and the other in the second. Furthermore, Arg68 could also possibly move in tandem with the Gln72 dyad, so as by swinging into conformation II it caused a conformational change in the Gln72 dyad, which in turn induced Arg68 from the neighboring subunit to rotate into conformation I. In this way, the release of a product in one subunit could allosterically facilitate water activation and subsequently deamination of a substrate in another subunit. An asymmetric dimer of such a structure has been reported in *Ec*CDA (*25*). Grown at 28 °C, this *Ec*CDA crystal structure showed one active site sequestered from the solvent while the other partially opened in the asymmetric unit. It is speculated that when one active site bound a product, the other would bind a substrate (*26*). The presence of both cytidine and uridine in the asymmetric unit of *Mm*CDA−cytidine might also lend support to such a mechanism. Nevertheless, *Ec*CDA does not share the same arginine and glutamine residues as *Mm*CDA, and hence it may have possessed a different mechanism for the subunits to alternate between the two states. Further investigations are necessary before a correct and detailed description of such an elegant mechanism can be offered.

Further Classification of Homotetrameric CDAs. Interestingly, sequence alignment of CDAs from certain bacteria, such as the aquatic *Caulobacter crescentus* and the radiation-resistant *Deinococcus radiodurans*, shows that Arg68 of *Mm*CDA is replaced with a glutamine residue (Figure 4). Since substituting Arg56 of *Bs*CDA with glutamine reduces its V_{max} (*7*), some complementary modifications in these enzymes, for example, potentially the Arg72 preceding the CAEQ motif in *D. radiodurans* CDA, may be expected to restore a balanced charge distribution between the three cysteine residues and the zinc ion. It is also plausible that these bacterial CDAs with such a glutamine residue were the precursor of the homodimeric CDA, as replacement of arginine with glutamine would have provided the necessary room required for the subsequent substitution of the zinc-coordinating cysteine with the larger histidine in the homodimeric CDA.

Equally notable is that Arg68 of *Mm*CDA is replaced with a hydrophobic Leu57 in the *At*BSD structure, but Ala101 of *Mm*CDA is swapped for Arg90 in the PCGRCRQ motif of *At*BSD (Figure 4). Instead of interacting directly with the cysteine residues, Arg90 of *At*BSD with one or two water molecules constructs an alternative hydrogen bond network for Cys54 and Cys91. Likewise, position swapping of arginine is also observed in the CDA sequences of certain mycobacteria such as *Mycobacterium leprae* and *Streptomyces coelicolor* (Figure 4). These observations suggest that homotetrameric CDAs can further be subclassified into CAER(Q) CDAs, which have the charge-neutralizing arginine (or glutamine) residue in the conserved CAER(Q) motif, and PCGRC CDAs, which have the corresponding arginine in the conserved PCGRCRQ motif. However, exception does exist as the *Methylobacterium chloromethanicum* CDA, perplexingly, has alanine in both sites (Figure 4).

Could MmCDA Be Also an RNA-Editing Deaminase? The yeast *Sc*CDD1, intriguingly, has been demonstrated to deaminate also the C6666 of apolipoprotein B (apoB) mRNA in addition to free cytidine (*10*). ApoB mRNA is a substrate of APOBEC1, a zinc-dependent cytidine deaminase homologous to *Ec*CDA (*26*, *27*) that converts a *C*AA codon to a *U*AA stop codon, thereby generating two isoforms of apoB protein (*28*). However, structural comparison of the uncomplexed *Sc*CDD1 (*8*) with *Mm*CDA clearly shows that the active site has enough space for only a free cytidine molecule but not one in an RNA molecule, although *Sc*CDD1 reportedly requires some auxiliary factors expressed in the yeast to edit apoB mRNA (*10*). Strikingly, CDA from the parasitic nematode *Brugia pahangi* (*Bp*CDD), but neither *Ec*CDA nor *Bs*CDA, has also been reported to bind to AU-rich RNA templates besides apoB RNA templates in the

presence of chicken S100 extract (*29*). Another two CDAs from the nematode *Caenorhabditis elegans*, *Ce*-CDD-1 and *Ce*-CDD-2, also exhibit RNA-binding activity toward AU-rich RNA templates but not an apoB RNA template (*30*). These RNA-interacting CDAs of eukaryotic origins could possibly play a novel role in RNA metabolism instead of the pyrimidine salvage pathway.

Although the four RNA-interacting CDAs do not display any apparent RNA-binding motifs, sequence alignment has revealed that two aromatic residues present in them, the first being either tyrosine or histidine (*Bp*CDD Tyr69, *Ce*-CDD-1 His76, *Ce*-CDD-2 Tyr76, *Sc*CDD1 His75) and the second phenylalanine (*Bp*CDD Phe98, *Ce*-CDD-1 Phe105, *Ce*-CDD-2 Phe105, *Sc*CDD1 Phe106), are replaced with linear residues in both *Ec*CDA and *Bs*CDA that do not bind RNAs (Figure 4). Aromatic residues are important for interaction with the bases of RNAs, as mutating the Phe66 and Phe87 of APOBEC1, two residues strictly conserved sometimes as tyrosine in the APOBEC family (*31*), to leucine abolished editing and UV cross-linking to RNA (*32*). In *Sc*CDD1, presently the only solved structure with reported RNA-interacting activity, the first aromatic residue, His75, is exposed to the solvent (Figure 3d) but the second, Phe106, is largely buried. His75 is not as highly conserved as Phe106 (Figure 4), implying that CDAs with such an aromatic residue, which also includes *Mm*CDA (Tyr79, Figure 3d) and *Hs*CDA (Tyr79), might have acquired an additional function of interacting with RNAs. On the other hand, the more widely conserved Phe106 might play only a structural role.

Given the close structural similarities with *Sc*CDD1, it may not be surprising if *Mm*CDA too could act on RNAs. *Sc*CDD1 is distributed in both the nucleus and cytoplasm (*10*), and *Hs*CDA has been demonstrated to be present in the nucleus (*33*). The N-terminal bipartite NLS identified in *Hs*CDA (*33*) is also shared by *Mm*CDA, indicating that *Mm*CDA could also be localized to the nucleus where editing of apoB mRNA occurs (*34*, *35*). A complete picture of the CDA functions will certainly necessitate characterizations of the RNA binding and editing mechanisms of these RNA-interacting CDAs.

CONCLUSION

The three crystal structures of *Mm*CDA have provided interesting insights into the CDA mechanism. The *Mm*CDA−DAU complex clearly shows that CDAs differentiate a substrate from others by the presence of a hydrogen bond donating group at the C4 of the pyrimidine moiety. Structural analysis of enzyme−substrate is also possible under certain crystallization conditions as demonstrated by the *Mm*CDA−cytidine complex. Furthermore, crystal packing may also possibly contribute a factor in substrate/product formation, giving rise to the heterogeneity observed in the *Mm*CDA−cytidine complex where cytidine was found to bind in three of the subunits and uridine in one.

The high resolution of the *Mm*CDA−THU, meanwhile, has revealed an Arg68 unambiguously in two alternate conformations, I and II. Arg68 forms two hydrogen bonds with the zinc-coordinating Cys65 and Cys102 in conformation I, partly compensating their negative charges in order to maintain the reactivity of the catalytic zinc ion for substrate deamination. In contrast, rotating the side chain of Arg68 by about 130° into conformation II abolishes these hydrogen bonds. This may indirectly weaken the zinc−product interaction by enhancing the negativity of the zinc electrostatic environment, therefore promoting product dissociation.

Positional swapping of Arg68 is observed in certain CDAs and *At*BSD, leading to the identification of two new subclasses of the homotetrameric CDA. Studies on four RNA-interacting CDAs also point to a possible role in RNA metabolism for certain homotetrameric CDAs from eukaryotes. Overall, these results further show that much still has to be learned about the mechanism, evolution, and diversification of CDA, an ever-present protein of a seemingly ancient origin.

REFERENCES

1. Cacciamani, T., Vita, A., Cristalli, G., Vincenzetti, S., Natalini, P., Ruggieri, S., Amici, A., and Magni, G. (1991) Purification of human cytidine deaminase: molecular and enzymatic characterization and inhibition by synthetic pyrimidine analogs, *Arch. Biochem. Biophys. 290*, 285−292.
2. Wisdom, G. B., and Orsi, B. A. (1967) Cytidine aminohydrolase from sheep liver, *Biochem. J. 104*, 7P.
3. Betts, L., Xiang, S., Short, S. A., Wolfenden, R., and Carter, C. W. J. (1994) Cytidine deaminase. The 2.3 Å crystal structure of an enzyme:transition-state analog complex, *J. Mol. Biol. 235*, 635−656.
4. Johansson, E., Mejlhede, N., Neuhard, J., and Larsen, S. (2002) Crystal structure of the tetrameric cytidine deaminase from *Bacillus subtilis* at 2.0 Å resolution, *Biochemistry 41*, 2563−2570.
5. Vincenzetti, S., Cambi, A., Neuhard, J., Schnorr, K., Grelloni, M., and Vita, A. (1999) Cloning, expression, and purification of cytidine deaminase from *Arabidopsis thaliana*, *Protein Expression Purif. 15*, 8−15.
6. Chung, S. J., Fromme, J. C., and Verdine, G. L. (2005) Structure of human cytidine deaminase bound to a potent inhibitor, *J. Med. Chem. 48*, 658−660.
7. Johansson, E., Neuhard, J., Willemoës, M., and Larsen, S. (2004) Structural, kinetic, and mutational studies of the zinc ion environment in tetrameric cytidine deaminase, *Biochemistry 43*, 6020−6029.
8. Xie, K., Sowden, M. P., Dance, G. S. C., Torelli, A. T., Smith, H. C., and Wedekind, J. E. (2004) The structure of a yeast RNA-editing deaminase provides insight into the fold and function of activation-induced deaminase and APOBEC-1, *Proc. Natl Acad. Sci. U.S.A. 101*, 8114−8119.
9. Yamaguchi, I., Shibata, H., Seto, H., and Misato, T. (1975) Isolation and purification of blasticidin S deaminase from *Aspergillus terreus*, *J. Antibiot. 28*, 7−14.
10. Dance, G. S. C., Beemiller, P., Yang, Y., Mater, D. V., Mian, I. S., and Smith, H. C. (2001) Identification of the yeast cytidine deaminase CDD1 as an orphan C→U RNA editase, *Nucleic Acids Res. 29*, 1772−1780.
11. Vagin, A., and Teplyakov, A. (1997) Molrep: an automated program for molecular replacement, *J. Appl. Crystallogr. 30*, 1022−1025.
12. Brunger, A. T., Adams, P. D., Clore, G. M., DeLano, W. L., Gros, P., Grosse-Kunstleve, R. W., Jiang, J.-S., Kuszewski, J., Nilges, M., Pannu, N. S., Read, R. J., Rice, L. M., Simonson, T., and Warren, G. L. (1998) Crystallography and NMR system: a new software suite for macromolecular structure determination, *Acta Crystallogr. D54*, 905−921.
13. McRee, D. (1999) XtalView/Xfit−a versatile program to manipulate atomic coordinates and electron density, *J. Struct. Biol. 125*, 156−165.
14. Painter, J., and Merritt, E. A. (2006) *TLSMD* web server for the generation of multi-group TLS models, *J. Appl. Crystallogr. 39*, 109−111.
15. Murshudov, G. N., Vagin, A. A., and Dodson, E. J. (1997) Refinement of macromolecular structures by the maximum-likelihood method, *Acta Crystallogr. D53*, 240−255.
16. Chenna, R., Sugawara, H., Koike, T., Lopez, R., Gibson, T. J., Higgins, D. G., and Thompson, J. D. (2003) Multiple sequence

alignment with the Clustal series of programs, *Nucleic Acids Res. 31*, 3497−3500.
17. Kraulis, P. J. (1991) MOLSCRIPT: a program to produce both detailed and schematic plots of protein structures, *J. Appl. Crystallogr. 24*, 946−950.
18. Merrit, E. A., and Bacon, D. J. (1997) Raster3D: photorealistic molecular graphics, *Methods Enzymol. 277*, 505−524.
19. Wilson, D. K., Rudolph, F. B., and Quiocho, F. A. (1991) Atomic structure of adenosine deaminase complexed with a transition-sate analog: understanding catalysis and immunodeficiency mutations, *Science 252*, 1278−1284.
20. Xiang, T. X., Niemi, R., Bummer, P., and Anderson, B. D. (2003) Epimer interconversion, isomerization, and hydrolysis of tetrahydrouridine: implications for cytidine deaminase inhibition, *J. Pharm. Sci. 92*, 2027−2039.
21. Xiang, S., Short, S. A., Wolfenden, R., and Carter, C. W. J. (1996) Cytidine deaminase complexed to 3-deazacytidine: a "valence buffer" in zinc enzyme catalysis, *Biochemistry 35*, 1335−1341.
22. Xiang, S., Short, S. A., Wolfenden, R., and Carter, C. W. J. (1997) The structure of the cytidine deaminase-product complex provides evidence for efficient proton transfer and ground-state destabilization, *Biochemistry 36*, 4768−4774.
23. Cohen, R. M., and Wolfenden, R. (1971) The equilibrium of hydrolytic deamination of cytidine and N^4-methylcytidine, *J. Biol. Chem. 246*, 7566−7568.
24. Cullis, P. M., and Wolfenden, R. (1981) Affinities of nucleic acid bases for solvent water, *Biochemistry 20*, 3024−3028.
25. Kuyper, L. F., and Carter, C. W. J. (1996) Resolving crystal polymorphisms by finding "stationary points" from quantitative analysis of crystal growth response surfaces, *J. Crystal Growth 168*, 155−169.
26. Navaratnam, N., Fujino, T., Bayliss, J., Jarmuz, A., How, A., Richardson, N., Somasekaram, A., Bhattacharya, S., Carter, C., and Scott, J. (1998) *Escherichia coli* cytidine deaminase provides a molecular model for ApoB RNA editing and a mechanism for RNA substrate recognition, *J. Mol. Biol. 275*, 695−714.
27. Navaratnam, N., Morrison, J. S., Bhattacharya, S., Patel, D., Funahashi, T., Giannoni, F., Teng, B. B., Davidson, N. O., and Scott, J. (1993) The p27 catalytic subunit of the apolipoprotein B mRNA editing enzyme is a cytidine deaminase, *J. Biol. Chem. 268*, 20709−20712.
28. Davidson, N. O. (1993) Apolipoprotein B mRNA editing: A key controlling element targeting fats to proper tissue, *Ann. Med. 25*, 539−543.
29. Anant, S., Martin, S. A. M., Yu, H., MacGinnitie, A. J., Devaney, E., and Davidson, N. O. (1997) A cytidine deaminase expressed in the post-infective L3 stage of the filarial nematode, *Brugia pahangi*, has a novel RNA-binding activity, *Mol. Biochem. Parasitol. 88*, 105−114.
30. Thompson, F. J., Britton, C., Wheatley, I., Maitland, K., Walker, G., Anant, S., Davidson, N. O., and Devaney, E. (2002) Biochemical and molecular characterization of two cytidine deaminases in the nematode *Caenorhabditis elegans*, *Biochem. J. 365*, 99−107.
31. Jarmuz, A., Chester, A., Bayliss, J., Gisbourne, J., Dunham, I., Scott, J., and Navaratnam, N. (2002) An anthropoid-specific locus of orphan C to U RNA-editing enzymes on chromosome 22, *Genomics 79*, 285−296.
32. Navaratnam, N., Bhattacharya, S., Fujino, T., Patel, D., Jarmuz, A. L., and Scott, J. (1995) Evolutionary origins of *apoB* mRNA editing: catalysis by a cytidine deaminase that has acquired a novel RNA-binding motif at its active site, *Cell 81*, 187−195.
33. Somasekaram, A., Jarmuz, A., How, A., Scott, J., and Navaratnam, N. (1999) Intracellular localization of human cytidine deaminase. Identification of a functional nuclear localization signal, *J. Biol. Chem. 274*, 28405−28412.
34. Lau, P. P., Xiong, W., Zhu, H.-T., Chen, S.-H., and Chan, L. (1991) Apolipoprotein B mRNA editing is an intranuclear event that occurs posttranscriptionally coincident with splicing and polyadenylation, *J. Biol. Chem. 266*, 20550−20554.
35. Yang, Y., Sowden, M. P., and Smith, H. C. (2000) Induction of cytidine to uridine editing on cytoplasmic apolipoprotein B mRNA by overexpressing APOBEC-1, *J. Biol. Chem. 275*, 22663−22669.

BI060345F